Available online at www.sciencedirect.com
ScienceDirect
Nuclear Physics B Proceedings Supplement 00 (2012) 1–6
Nuclear Physics B Proceedings Supplement

Heavy Flavour Cross Section Measurements with the ATLAS Detector

Chris Hawkes, on behalf of the ATLAS Collaboration

School of Physics and Astronomy, University of Birmingham, Birmingham, B15 2TT, United Kingdom

Abstract

ATLAS measurements of heavy flavour production cross sections are presented from proton-proton collisions at the LHC at a centre-of-mass energy of 7 TeV. These make use of b-hadron decays to $D^*\mu X$, inclusive charm meson production, inclusive electron and muon production from semileptonic heavy flavour decays, and reconstruction of secondary decay vertices to tag b-jets. The results are compared with next-to-leading-order QCD calculations.

Keywords: flavour physics, heavy quark production, B physics, QCD

1. Introduction and motivation

Heavy flavour production has been measured at hadron colliders for many years, for example in proton-antiproton collisions at centre-of-mass energies of $\sqrt{s}$ = 0.63, 1.8 and 1.96 TeV at the Sp$\bar{\text{p}}$S [1] and Tevatron [2, 3] colliders. The predicted cross sections for heavy flavour production have also been available for many years [4], calculated using next-to-leading-order perturbative quantum chromodynamics (NLO QCD). Nevertheless, there are large theoretical uncertainties, notably due to the dependence on the choice of the renormalisation and factorisation scales. It is therefore of interest to measure heavy flavour cross sections at the much higher centre-of-mass energies of proton-proton collisions at the Large Hadron Collider (LHC). This provides an opportunity to test NLO QCD calculations in a new energy range and helps to constrain the theoretical uncertainties.

In addition to its intrinsic interest, heavy flavour production in the Standard Model (SM) creates an important background to many of the searches for new phenomena that are being performed at the LHC. Measurements of the heavy flavour cross sections lead to a better understanding of this source of background and hence improve the sensitivity of these searches.

ATLAS has measured heavy flavour production in pp collisions at $\sqrt{s}$ = 7 TeV. Four techniques are used: reconstruction of b-hadrons decaying to $D^*\mu X$, inclusive charm meson production, inclusive lepton production, as a tag of semileptonic heavy flavour decays, and reconstruction of secondary decay vertices to tag b-jets. The results are compared with NLO QCD predictions.

2. The ATLAS detector

ATLAS [5] is a general-purpose detector covering almost the full solid angle. These measurements make use of the charged-particle tracking and vertex reconstruction within the pseudorapidity range $|\eta| < 2.5$ provided by the inner detector. This consists of a silicon pixel detector, a silicon microstrip tracker and a transition radiation tracker, all inside a 2 T axial magnetic field. Some analyses also make use of muon identification with the muon spectrometer and electron identification by the calorimeters and transition radiation tracker.

These heavy flavour analyses require a relatively loose trigger, which ATLAS was able to use during the early stages of data-taking at $\sqrt{s}$ = 7 TeV, when the instantaneous luminosity was low and the rate of multiple interactions per bunch crossing was not too high. As the LHC luminosity increased, the trigger criteria had to be tightened or the trigger prescaled. Consequently, the results presented in this paper are based only on the data recorded by ATLAS in 2010, and in some cases only a small subset of the 2010 data.

3. Decays of b-hadrons to $D^*\mu X$ final state

ATLAS has measured the inclusive cross section for the production of hadrons containing a b quark (H_b) by partial reconstruction of their semileptonic decays: $H_b \to D^{*+}\mu^- X$, with $D^{*+} \to D^0\pi^+$ and $D^0 \to K^-\pi^+$ [6].

An identified muon is required, which has to trigger the event, together with three tracks of the appropriate charges to allow full reconstruction of the D^* decay. A simultaneous fit is made to the decay vertices of the b-hadron and the D^0. The kinematic acceptance is defined by selection cuts on the transverse momentum and pseudorapidity of the D^* and the muon: $p_{\rm T}(D^*) > 4.5$ GeV and $|\eta(D^*)| < 2.5$, and $p_{\rm T}(\mu) > 6$ GeV and $|\eta(\mu)| < 2.4$.

The differential cross section is defined as:

$$\frac{d\sigma\,(pp \to H_b X \to D^{*+}\mu^- X')}{dp_{\rm T}\,(D^*\mu)} = \frac{f_b\,N(D^*\mu)}{2\epsilon\,\mathcal{B}\mathcal{L}\,\Delta p_{\rm T}}\,.$$

The number of reconstructed $D^*\mu$ pairs observed, $N(D^*\mu)$, must be corrected by $f_b = (93.2 \pm 0.3)\,\%$, the fraction of $D^*\mu$ pairs that originate from signal b-hadron decays, as determined from Monte Carlo simulation (MC), and by the efficiency, ϵ. The latter consists of three components: the efficiency for reconstructing the $D^*\mu$ signal within the kinematic acceptance (48.3%), and the efficiency of the $H_b \to D^*\mu X$ selection (79.1%), both of which are found from MC, and the single-muon trigger efficiency (81.9%), which is measured using an independent control sample of $J/\psi \to \mu^+\mu^-$ decays. Both charge-conjugate pairs, $D^{*+}\mu^-$ and $D^{*-}\mu^+$, are counted in $N(D^*\mu)$ and so a factor of two is required in the denominator to give the cross section for a hadron containing a b (rather than a $\bar{b}$) quark. The other factors are the product branching fraction, $\mathcal{B} = \mathcal{B}\left(D^{*+} \to D^0\pi^+\right)\mathcal{B}\left(D^0 \to K^-\pi^+\right) = 2.63\%$, the integrated luminosity, $\mathcal{L} = 3.3$ pb^{-1}, and the bin width, $\Delta p_{\rm T}$.

This measured differential cross section as a function of $p_{\rm T}\,(D^*\mu)$ is corrected to account for the kinematics of the unreconstructed particles, X, and yields the differential cross section as a function of the b-hadron momentum, $p_{\rm T}(H_b)$. Finally, to extract the b-hadron production cross section, the accepted kinematic region is redefined to be $p_{\rm T}(H_b) > 9$ GeV and $|\eta(H_b)| < 2.5$. A bin-by-bin acceptance correction is applied and the result is divided by $\mathcal{B}\,(H_b \to D^{*+}\mu^- X) = (2.75 \pm 0.19)\,\%$ to give $d\sigma\,(pp \to H_b X)/dp_{\rm T}\,(H_b)$, which is shown in Fig. 1, together with the differential cross section as a function of $|\eta(H_b)|$. The experimental systematic uncertainties have large variations with $p_{\rm T}$ and $|\eta|$. They are dominated by the use of NLO QCD MC to calculate the kinematics and acceptance corrections (1-30%) and also the reconstruction and selection efficiencies (10-15%).

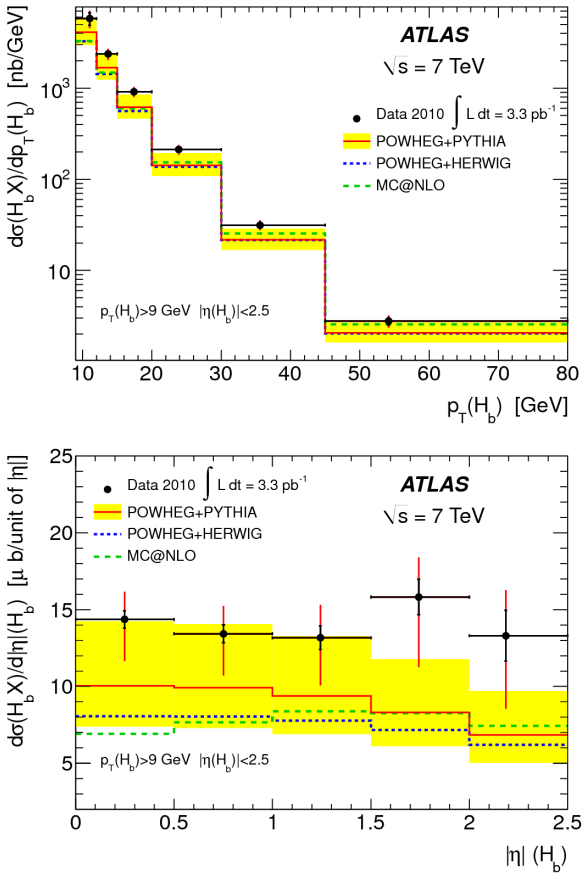

Figure 1: Differential cross sections for b-hadron production as functions of $p_{\rm T}(H_b)$ and $|\eta(H_b)|$ [6] compared to theoretical predictions. The inner error bars show the statistical uncertainties, the outer error bars the total experimental uncertainties and the shaded bands the theoretical uncertainties.

The measurements are compared with NLO QCD predictions calculated using POWHEG-HVQ 1.01 [7] combined with either PYTHIA 6.4 [8] or HERWIG 6.5 [9], which are used to simulate the parton shower, and with MC@NLO 4.0 [10] combined with HERWIG 6.5. The predictions are lower than the data, but consistent given the theoretical uncertainties, which are dominated by the scale uncertainties.

Integrating the differential cross section gives the b-hadron production cross section measured within the kinematic range $p_{\rm T}(H_b) > 9$ GeV and $|\eta(H_b)| < 2.5$:

$$\sigma(pp \to H_b X) = 32.7 \pm 0.8\,(\text{stat.}) \pm 3.1\,(\text{syst.}) \\ {}^{+2.1}_{-5.6}(\text{accept.}) \pm 2.3(\mathcal{B}) \pm 1.1(\mathcal{L})\ \mu\text{b}\,,$$

where the last three uncertainties come from the accep-

tance correction, the branching fractions and the luminosity, respectively.

The b-hadron production cross section predicted by POWHEG+PYTHIA is:

$$\sigma(pp \to H_b X) = 22.2\,^{+8.9}_{-5.4}\,(\text{scale})\,^{+2.1}_{-1.9}\,(m_b)\,^{+2.2}_{-2.1}\,(\text{PDF})\,^{+1.6}_{-1.5}\,(\text{hadr.})\,\mu\text{b}\,,$$

where the theoretical uncertainties come from variation of the renormalisation and factorisation scales, the b-quark mass, the proton parton distribution function, and the heavy quark hadronisation model. The equivalent predictions from POWHEG+HERWIG and MC@NLO are 18.6 μb and 19.2 μb, respectively, with similar theoretical uncertainties. They are all lower than the data, but consistent within the uncertainties.

To produce a total cross section that can be compared directly with measurements made by other experiments, the ATLAS result is extrapolated to the full phase space region using the NLO QCD MC calculation, which requires multiplying by a factor of $11.0^{+2.6}_{-1.6}$:

$$\sigma(pp \to H_b X)_{\text{total}} = 360 \pm 9(\text{stat.}) \pm 34(\text{syst.}) \pm 25(\mathcal{B}) \pm 12(\mathcal{L})^{+77}_{-69}(\text{accept.} \oplus \text{extrap.})\,\mu\text{b}\,,$$

where the final uncertainty comes from the combined acceptance and extrapolation corrections. This can be compared with three other LHC measurements of the inclusive $b\bar{b}$ cross section in $\sqrt{s}$ = 7 TeV pp collisions, extrapolated to the full phase space region. LHCb measures 284 ± 20 (stat.) ± 49 (syst.) μb [11] from $H_b \to D^0\mu X$ decays, extrapolated from $2 < \eta < 6$, and 288 ± 4 (stat.) ± 48 (syst.) μb [12] from $H_b \to J/\psi\, X$ decays, extrapolated from the rapidity range $2.0 < y < 4.5$. ALICE measures $244 \pm 64\,(\text{stat.})\,^{+50}_{-59}\,(\text{syst.})\,^{+7}_{-6}\,(\text{extrap.})$ μb [13] from $H_b \to J/\psi\, X$ decays, extrapolated from $p_{\text{T}} > 1.3$ GeV and $|y| < 0.9$. The ATLAS measurement is somewhat higher than the others, but they are all consistent within the quoted uncertainties.

CMS has also measured the cross sections at $\sqrt{s}$ = 7 TeV for B^+ [14], B^0 [15], B^0_s [16] and Λ_b [17] production, while LHCb has measured the B^+ production cross section in the forward region [18].

4. Inclusive charm meson production

Inclusive production of charm mesons at the LHC is sensitive to both c and b quark production and fragmentation, with about 10% expected to originate from b-hadron decays. ATLAS has preliminary measurements of the differential cross sections for charged D^*, D and D_s production [19] within the kinematic range $p_{\text{T}} > 3.5$ GeV and $|\eta| < 2.1$. In this analysis, charm mesons are reconstructed from fully hadronic decay modes, so there is no lepton to trigger the events, and therefore a minimum-bias trigger is used. This restricts the analysis to 1.1 nb^{-1} from the early 2010 running, after accounting for prescale factors, but there are ample statistics to measure the large cross sections.

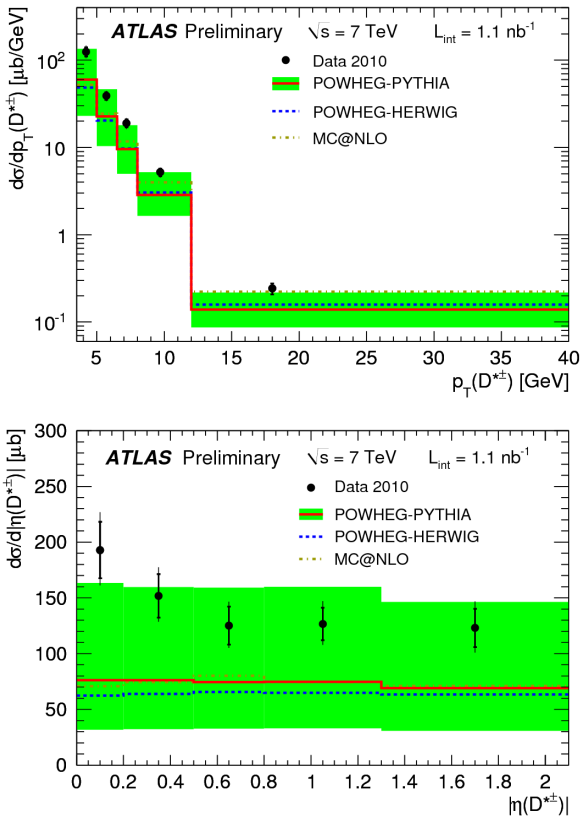

Figure 2: Differential cross sections for $D^{*\pm}$ production as functions of $p_{\text{T}}(D^*)$ and $|\eta(D^*)|$ [19] compared to theoretical predictions. The inner error bars show the statistical uncertainties and the outer error bars show the total experimental uncertainties. The shaded band shows the theoretical uncertainty.

Selection cuts for the charm mesons were tuned using MC events and exploit the high p_{T} decay products from hard charm fragmentation, the displaced secondary vertices from the long $D^{(*)}$ meson lifetimes and the angular distributions resulting from their spins. All fitted masses and widths are consistent with expectations.

Differential cross sections for $D^{*\pm}$ and $D^{\pm}$ production as functions of p_{T} and $|\eta|$ are shown in Fig. 2 and Fig. 3, respectively. The data are compared with three sets of NLO QCD predictions, all of which lie below the measured values, but they are consistent within the large uncertainties.

These ATLAS differential cross section measure-

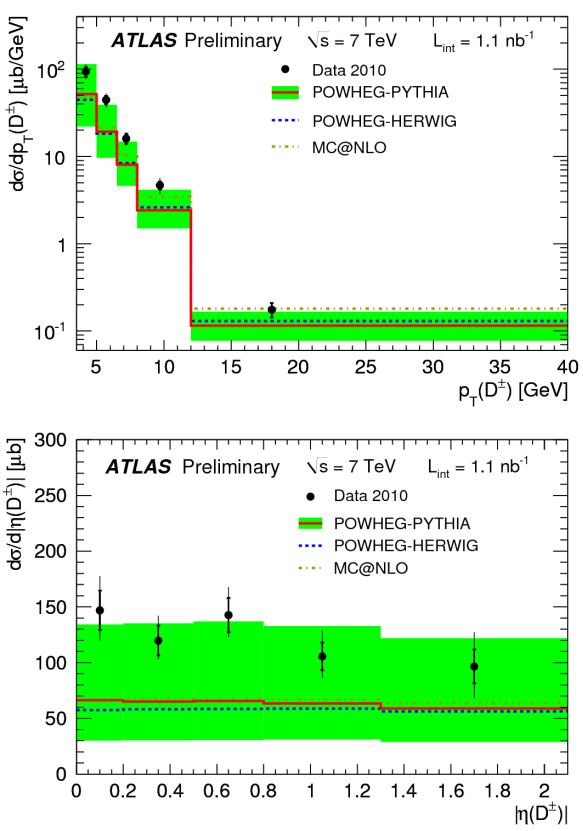

Figure 3: Differential cross sections for $D^{\pm}$ production as functions of $p_{\mathrm{T}}(D)$ and $|\eta(D)|$ [19] compared to theoretical predictions. Inner error bars show statistical uncertainties, outer error bars the total experimental uncertainties and the shaded band the theoretical uncertainty.

ments have also been compared with two other sets of NLO QCD calculations [20]. The predictions of the Fixed-Order Next-to-Leading-Log (FONLL) scheme [21] are higher than those of POWHEG or MC@NLO, but still below the data, while predictions in the General-Mass Variable-Flavor-Number Scheme [22] are slightly above, but consistent with, the data.

The integrated cross sections measured by ATLAS within $p_{\mathrm{T}} > 3.5$ GeV and $|\eta| < 2.1$ are:

$$\sigma(D^{*\pm}) = 285 \pm 16\,(\mathrm{stat.})^{+32}_{-27}(\mathrm{syst.}) \pm 31(\mathcal{L}) \pm 4(\mathcal{B})\ \mu\mathrm{b}\ ,$$

$$\sigma(D^{\pm}) = 238 \pm 13\,(\mathrm{stat.})^{+35}_{-23}(\mathrm{syst.}) \pm 26(\mathcal{L}) \pm 10(\mathcal{B})\ \mu\mathrm{b}\ ,$$

$$\sigma(D^{\pm}_{s}) = 168 \pm 34\,(\mathrm{stat.})^{+27}_{-25}(\mathrm{syst.}) \pm 18(\mathcal{L}) \pm 10(\mathcal{B})\ \mu\mathrm{b}\ .$$

The POWHEG+PYTHIA predictions are:

$$\sigma(D^{*\pm}) = 153^{+169}_{-80}(\mathrm{scale})^{+13}_{-15}(m_Q)^{+24}_{-21}(\mathrm{PDF})^{+20}_{-16}(\mathrm{hadr.})\,\mu\mathrm{b}\ ,$$

$$\sigma(D^{\pm}) = 132^{+137}_{-65}(\mathrm{scale})^{+11}_{-10}(m_Q)^{+20}_{-18}(\mathrm{PDF})^{+21}_{-11}(\mathrm{hadr.})\,\mu\mathrm{b}\ ,$$

$$\sigma(D^{\pm}_{s}) = 59^{+57}_{-28}(\mathrm{scale})^{+4}_{-6}(m_Q)^{+9}_{-8}(\mathrm{PDF})^{+7}_{-8}(\mathrm{hadr.})\,\mu\mathrm{b}\ ,$$

which are lower than, but consistent with, the data.

Consistent measurements of charm meson production at central rapidity have been made by ALICE [23].

5. Inclusive lepton cross sections

ATLAS has measured the inclusive production of electrons and muons from the semileptonic decays of hadrons containing heavy quarks [24]. Leptons from heavy flavour, W and Z decays can be separated from other background sources, such as photon conversions, decays in flight of pions and kaons and hadronic jets faking electron signals, using various discriminating variables. Decays of W and Z bosons populate the high p_{T} region, while leptons from heavy flavour decays are concentrated at lower p_{T}. Subtracting the SM contribution from W and Z decays yields the cross section from heavy flavour decays.

Figure 4 shows the ATLAS inclusive muon differential cross section from heavy flavour production as a function of $p_{\mathrm{T}}(\mu)$, compared to several NLO QCD predictions. The data agree with the POWHEG+PYTHIA and FONLL calculations, while POWHEG+HERWIG predicts a lower cross section. The data at high p_{T} deviate significantly from the FONLL curve if only the NLO term is included, but agree with the full FONLL calculation, showing the sensitivity of the measurement to the additional NLL resummation term.

CMS has also measured the inclusive production of b-hadrons with muons [25] and of $b\bar{b}X$ decaying to muons [26], and ALICE has measured heavy flavour decay muons at forward rapidity [27].

6. Measurements using b-jet tagging

This technique exploits the long lifetime of b-hadrons by looking for secondary decay vertices in hadronic jets that are significantly displaced from the primary pp vertex. The decay length significance is evaluated, by dividing the distance between primary and secondary vertices by its uncertainty. This is required to be greater than a certain value to define a b-tagged sample. The number of true b-jets within this sample is found by making a fit to the distribution of the invariant mass of the charged particles forming the secondary vertex. Templates for b-jets, charm jets and light-flavoured jets are taken from MC and their relative contributions varied in a fit to the data. These measurements are important for understanding the SM background to new

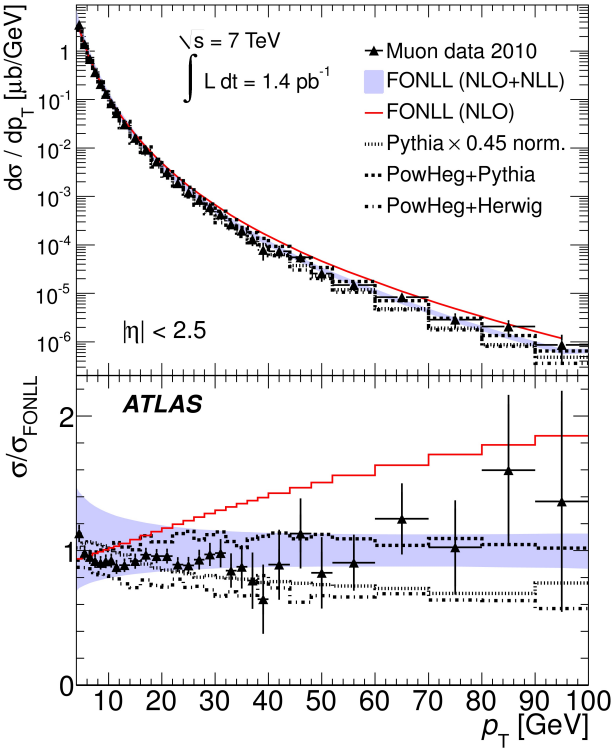

Figure 4: Muon differential cross section from heavy flavour production as a function of $p_{\mathrm{T}}(\mu)$ [24]. The lower plot shows the ratios of cross sections to calculations in the FONLL scheme [21]. The shaded region shows the theoretical uncertainty. Pythia is a lowest-order (LO) generator and is therefore not expected to predict the correct integrated cross section. It is normalised to the data to allow the shapes to be compared.

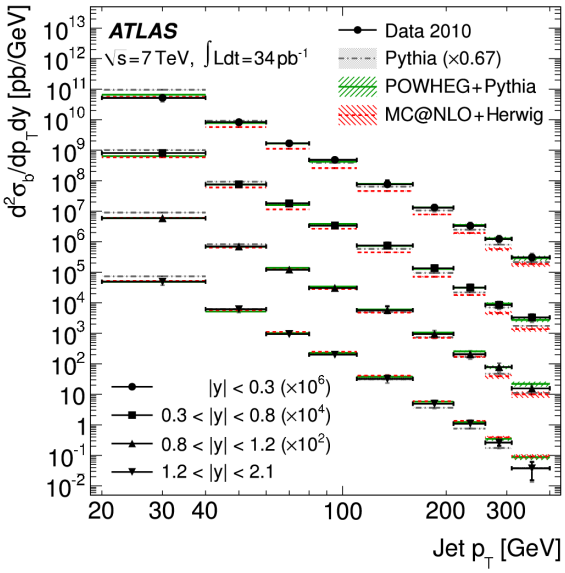

Figure 5: Inclusive b-jet double-differential cross section as a function of jet p_{T} for different rapidity ranges [28], compared to theoretical calculations. The Pythia LO prediction is normalised to the data.

particle searches, since b-jet tagging is often used as a signature in these searches.

Figure 5 shows the ATLAS inclusive double-differential cross section for b-jet production [28] as a function of jet p_{T} for four different ranges of rapidity. Measurements are compared to three NLO QCD calculations, which describe the general features of the data, but MC@NLO+HERWIG shows significant differences in the detailed dependence on p_{T} and $|y|$. CMS results on inclusive b-jet production [29] are similar.

Figure 6 shows the ATLAS inclusive $b\bar{b}$-dijet differential cross section [28] as a function of dijet invariant mass. The NLO QCD predictions agree with the measurements within the statistical uncertainties.

The same technique has been used to measure the production of a b-jet, with $p_{\mathrm{T}} > 25$ GeV and $|y| < 2.1$, in association with a Z or W boson, identified by its decay into high p_{T} leptons. ATLAS measures the cross section for producing a b-jet with a Z boson to be $3.55\,^{+0.82}_{-0.74}(\mathrm{stat.})\,^{+0.73}_{-0.55}(\mathrm{syst.}) \pm 0.12(\mathcal{L})$ pb [30], which is consistent with three NLO QCD predictions based on different models of heavy flavour production: 3.88 ± 0.58 pb from MCFM 5.8 [31], 2.23 ± 0.01 (stat. only) pb from ALPGEN 2.13 [32], and 3.29 ± 0.04 (stat. only) pb from SHERPA 1.1.3 [33]. There is better agreement with MCFM and SHERPA, which create a b-quark from the proton parton density function, whereas ALPGEN creates a $b\bar{b}$ pair from the gluon distribution. CMS has similar measurements of Z/γ^*+b-jet production [34].

Figure 7 shows ATLAS cross section measurements for production of a W boson, together with one or two jets, at least one of which is identified as a b-jet, but excluding top quark decays [35]. The NLO QCD calculations [8, 32, 36] are consistent with the data.

7. Summary

ATLAS has measured heavy flavour production cross sections in pp collisions at $\sqrt{s} = 7$ TeV at the LHC, using b-hadron decays to the $D^*\mu X$ final state, inclusive charm meson production, inclusive lepton production from semileptonic heavy flavour decays, and reconstruction of secondary decay vertices to tag b-jets. Results are consistent with NLO QCD predictions within theoretical uncertainties, which are dominated by renormalisation and factorisation scale uncertainties.

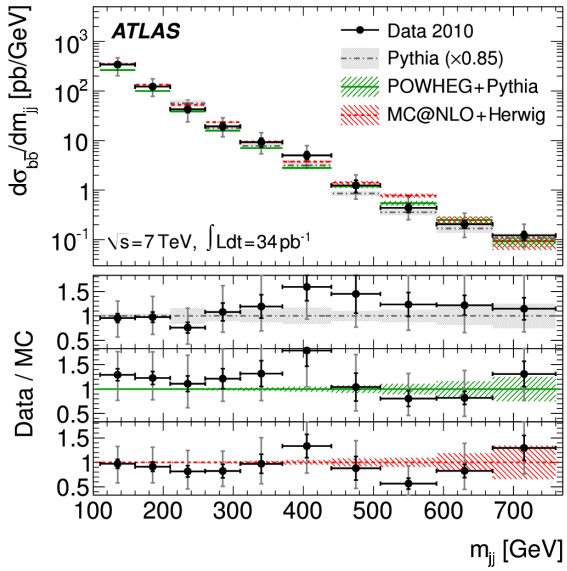

Figure 6: Cross section for $b\bar{b}$-dijet production as a function of dijet invariant mass, for b-jets with $p_{\mathrm{T}} > 40$ GeV and $|y| < 2.1$ [28], compared to theoretical calculations. The Pythia LO prediction is normalised to the data. Shaded regions show the statistical uncertainty only.

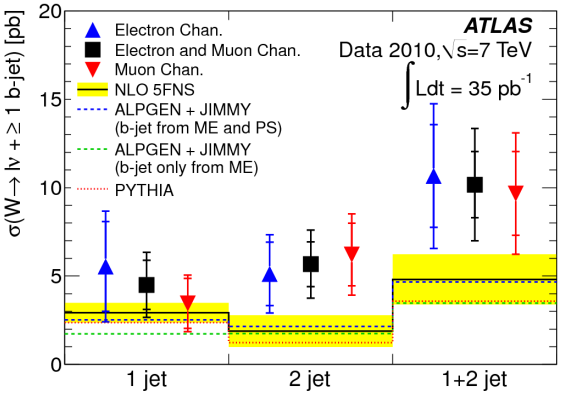

Figure 7: Cross sections for production of a W boson in association with one or two jets, at least one of which is a b-jet [35], but excluding top quark decays, compared with theoretical predictions [8, 32, 36]. The inner error bars show the statistical uncertainties, the outer error bars the total experimental uncertainties and the shaded band the theoretical uncertainty.

Acknowledgements

I am grateful for the funding provided by the United Kingdom Science and Technology Facilities Council and to the conference organisers for their invitation and hospitality.

References

[1] UA1 Collaboration, Phys. Lett. B186 (1987) 237;
Phys. Lett. B213 (1988) 405; Phys. Lett. B256 (1991) 121.
[2] CDF Collaboration, Phys. Rev. Lett. 71 (1993) 500;
Phys. Rev. Lett. 71 (1993) 2396; Phys. Rev. Lett. 75 (1995) 1451;
Phys. Rev. D65 (2002) 052005; Phys. Rev. D66 (2002) 032002;
Phys. Rev. D71 (2005) 032001; Phys. Rev. D75 (2007) 012010;
Phys. Rev. D79 (2009) 052008; Phys. Rev. D79 (2009) 092003;
Phys. Rev. Lett. 104 (2010) 131801.
[3] D0 Collaboration, Phys. Rev. Lett. 74 (1995) 3548;
Phys. Rev. Lett. 84 (2000) 5478; Phys. Lett. B487 (2000) 264;
Phys. Rev. Lett. 85 (2000) 5068; Phys. Rev. D83 (2011) 031105.
[4] P. Nason, S. Dawson. R.K. Ellis, Nucl. Phys. B303 (1988) 607;
Nucl. Phys. B327 (1989) 49.
[5] ATLAS Collaboration, JINST 3 (2008) S08003.
[6] ATLAS Collaboration, Nucl. Phys. B864 (2012) 341.
[7] P. Nason, JHEP 0411 (2004) 040;
S. Frixione, P. Nason, G Ridolfi, JHEP 0709 (2007) 126;
S. Frixone, P. Nason, C. Oleari, JHEP 0711 (2007) 070;
S. Alioli et al., JHEP 1006 (2010) 043.
[8] T. Sjöstrand, S. Mrenna, P.Z. Skands, JHEP 0605 (2006) 026.
[9] G. Corcella et al., JHEP 0101 (2001) 010.
[10] S. Frixione, B.R. Webber, JHEP 0206 (2002) 029;
S. Frixione, P. Nason, B.R. Webber, JHEP 0308 (2003) 007.
[11] LHCb Collaboration, Phys. Lett. B694 (2010) 209.
[12] LHCb Collaboration, Eur. Phys. J. C71 (2011) 1645.
[13] ALICE Collaboration, arXiv:1205.5880, submitted to JHEP.
[14] CMS Collaboration, Phys. Rev. Lett. 106 (2011) 112001.
[15] CMS Collaboration, Phys. Rev. Lett. 106 (2011) 252001.
[16] CMS Collaboration, Phys. Rev. D84 (2011) 052008.
[17] CMS Collaboration, Phys. Lett. B714 (2012) 136.
[18] LHCb Collaboration, JHEP 1204 (2012) 093.
[19] ATLAS Collaboration, ATLAS-CONF-2011-017,
https://cdsweb.cern.ch/record/1336746.
[20] ATLAS Collaboration, ATLAS-PHYS-PUB-2011-012,
https://cdsweb.cern.ch/record/1378479.
[21] M. Cacciari, M. Greco, P. Nason, JHEP 9805 (1998) 007;
M. Cacciari, P. Nason, JHEP 0309 (2003) 006;
M. Cacciari et al., JHEP 0407 (2004) 033.
[22] B.A. Kniehl et al., Phys. Rev. D71 (2005) 014018;
Phys. Rev. Lett. 96 (2006) 012001;
Phys. Rev. D79 (2009) 094009.
[23] ALICE Collaboration, JHEP 1201 (2012) 128.
[24] ATLAS Collaboration, Phys. Lett. B707 (2012) 438.
[25] CMS Collaboration, JHEP 1103 (2011) 090.
[26] CMS Collaboration, JHEP 1206 (2012) 110.
[27] ALICE Collaboration, Phys. Lett. B708 (2012) 265.
[28] ATLAS Collaboration, Eur. Phys. J. C71 (2011) 1846.
[29] CMS Collaboration, JHEP 1204 (2012) 084.
[30] ATLAS Collaboration, Phys. Lett. B706 (2012) 295.
[31] J.M. Campbell, R. Ellis,
Nucl. Phys. Proc. Suppl. 205-206 (2010) 10.
[32] M.J. Mangano et al., JHEP 0307 (2003) 001.
[33] T. Gleisberg et al., JHEP 0902 (2009) 007.
[34] CMS Collaboration, JHEP 1206 (2012) 126.
[35] ATLAS Collaboration, Phys. Lett. B707 (2012) 418.
[36] J.M. Campbell et al., Phys. Rev. D86 (2012) 034021;
J.M. Butterworth, J.R. Forshaw, M.H. Seymour,
Z. Phys. C72 (1996) 637.